Theoretical study of planar defects in silicon carbide

2002 J. Phys.: Condens. Matter 14 12733

(http://iopscience.iop.org/0953-8984/14/48/310)

INSTITUTE OF PHYSICS PUBLISHING JOURNAL OF PHYSICS: CONDENSED MATTER

J. Phys.: Condens. Matter **14** (2002) 12733–12740 PII: S0953-8984(02)54133-3

Theoretical study of planar defects in silicon carbide

Hisaomi Iwata[1,2], **Ulf Lindefelt**[1,2,3], **Sven Öberg**[4] **and Patrick R Briddon**[5]

[1] Department of Physics and Measurement Technology, Linköping University, SE-58183 Linköping, Sweden
[2] Department of Microelectronics and Information Technology, Royal Institute of Technology, KTH Electrum 229, SE-16440 Kista, Sweden
[3] ABB Group Services Centre, Corporate Research, SE-72178 Västerås, Sweden
[4] Department of Mathematics, Luleå University of Technology, SE-97187 Luleå, Sweden
[5] Department of Physics, University of Newcastle upon Tyne, Newcastle upon Tyne NE1 7RU, UK

Received 1 October 2002
Published 22 November 2002
Online at stacks.iop.org/JPhysCM/14/12733

Abstract

We report on a theoretical investigation of extended planar defects in 3C-, 4H-, 6H-, and 15R-SiC which can be formed without breaking any bonds, covering a wide range of planar defects: twin boundaries, stacking faults, and polytype inclusions. Their electronic structures have been intensively studied using an *ab initio* supercell approach based on the density functional theory. Stacking fault energies are also calculated using both the supercell method and the axial next-nearest-neighbour Ising model. We discuss the electronic properties and energies of these defects in terms of the geometrical differences of stacking patterns.

1. Introduction

Stacking faults (SFs) are significantly important crystal defects in SiC. The electrical degradation problem of the SiC-based bipolar devices in connection with the occurrence of SFs was discovered rather recently [1, 2]. Then, the electronic properties and their impact on the bipolar devices were investigated using a first-principles band-structure calculation by us [3], and, almost at the same time, a similar conclusion was also drawn by Miao *et al* [4]. We discovered that certain types of SF in 4H- and 6H-SiC give rise to *electrically active* states in the fundamental band gap at around 0.2 eV below the conduction band minima (CBM). These states can be interpreted as planar quantum wells (QWs), in which electrons can drift freely along the SF planes. The electronic properties of cubic inclusions (CIs) in 4H-SiC, which correspond to multiple SFs in neighbouring planes, have also been examined lately [5]. Our results seem to be fully consistent with recent experimental studies on this issue [6–12]. In this work, we have also studied the electronic properties of SFs in 15R-SiC and twin boundaries (TBs) in 3C-SiC.

We report on the nature of the planar defects which can be created without breaking any bonds and without inserting or extracting any atomic layers. As will be discussed, there exist a great variety of extended defects of this type in SiC (see figure 1). In the light of the geometrical differences of the stacking sequences, an assembly of studies on each planar defect is combined into a big picture.

2. Computational and analytical tools

2.1. Ab initio supercell method

The density functional theory (DFT) in the local density approximation is employed, where the wavefunctions are expanded in a basis containing s-, p-, and d-symmetry Gaussian orbitals and the charge density is described in a plane-wave basis. As to ion–electron interactions, norm-conserving pseudopotentials are used. The calculations are performed using a supercell technique with N atoms per supercell ($N = 96$ for SFs in 3C-, 4H-, 6H-SiC, and CIs in 4H-SiC; $N = 120$ for SFs in 15R-SiC and TBs in 3C-SiC). Therefore, these planar defects artificially repeat after N atomic layers along the c-axis, and spread infinitely perpendicular to the c-axis. Essentially, these supercell sizes are sufficiently large to rule out artificial defect–defect interactions [3, 5, 13].

We have not attempted to obtain any accurate band gap; therefore all the calculated band gaps are underestimated. This underestimate is a well-known failure of the DFT. However, experience shows that except for the underestimate of the band gap of semiconductors, the DFT gives quite accurate band structures including band separations, curvatures, etc.

2.2. The ANNNI model and QW analysis

In addition to the *ab initio* calculations, the axial next-nearest-neighbour Ising (ANNNI) model [14] up to the third-nearest-neighbour interactions is also used to calculate the SF energies in 3C-, 4H-, 6H-, and 15R-SiC. The ANNNI model is an approximation in the sense that this model concerns bilayer–bilayer interactions only up the nth-nearest-neighbour planes and cannot distinguish between a pair of geometrically different structures related through an interchange of Si and C atoms. However, the ANNNI model serves as a check of the numerical accuracy of the SF energies obtained by the *ab initio* supercell method.

To clarify the QW-like features of certain planar defects, we analyse the wavefunctions and Kohn–Sham eigen-energies using a simple rectangular one-dimensional QW model as shown in figure 2. The width and depth of the QWs correspond to the thickness of the 3C-like region and the conduction band offset (CBO) between the 3C- and the host polytype, respectively [5, 13].

3. Geometry of TBs, SFs, and polytype inclusions

This study has been limited to SFs of the glide type, which can be introduced by displacing the upper part of a crystal relative to the lower part at a certain (0001) basal plane of the glide type. A mechanism for the creation of these SFs is the motion of partial dislocations, which leave behind a stacking error [3, 13, 15]. The propagation of partial dislocations on (0001) basal planes is quite generally observed in the SiC-based bipolar devices, although the mechanism has not been understood yet with full certainty [1–13]. We have inspected all the possible geometrical configurations of SFs within this scheme and found that there are one, two, three, and five geometrically distinguishable SFs in 3C-, 4H-, 6H-, and 15R-SiC,

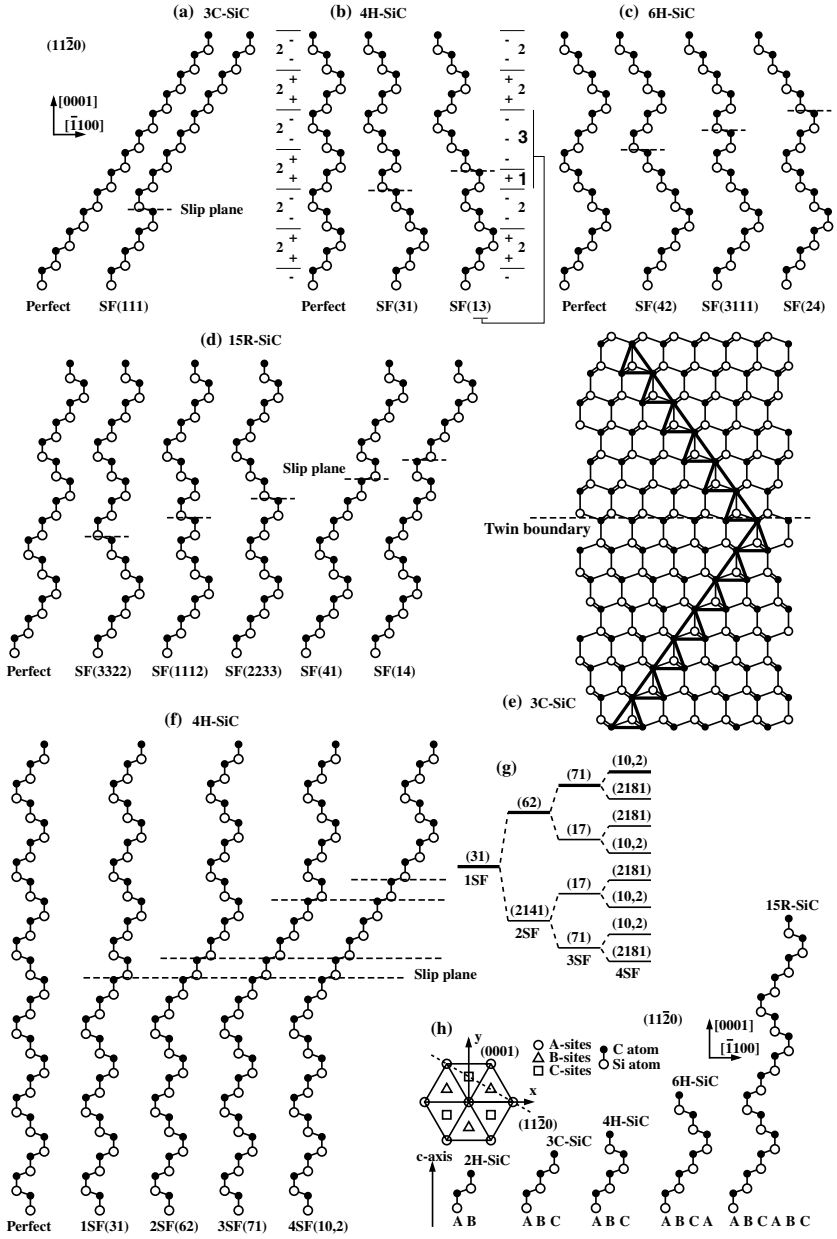

Figure 1. Schematic illustrations of the stacking sequences of the planar defects viewed from a [11$\bar{2}$0] direction (the [1$\bar{1}$0] direction in the cubic symmetry). Geometrically distinguishable SFs obtained by glide in (a) 3C-, (b) 4H-, (c) 6H-, and (d) 15R-SiC are shown as well as (e) a TB in 3C-SiC and (f) a subset of CIs in 4H-SiC corresponding to two, three, and four SFs together with (g) a tree diagram of the possible structures of the CIs. A tetrahedral stacking sequence is also shown for the TB in 3C-SiC. The notation system of the planar defects is explained using SF(13) in 4H-SiC. (h) Stacking sequences of the five common polytypes are also illustrated in terms of the ABC notation.

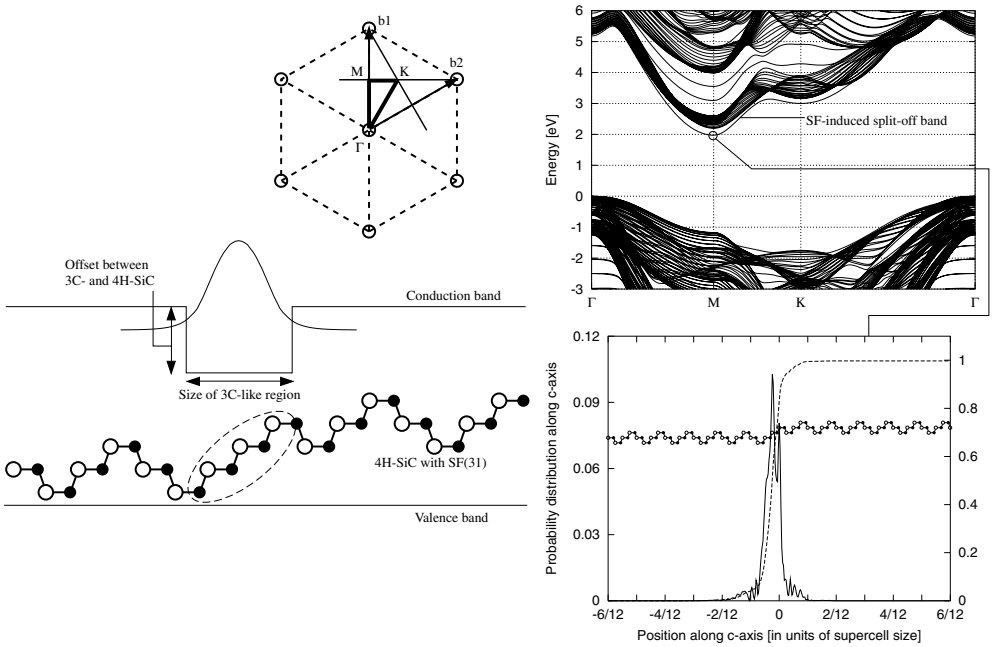

Figure 2. Schematic illustrations of QW features. High-symmetry lines in reciprocal space (upper left), a simple QM model for the SF structure (lower left), the two-dimensional band structure of the 96-atom supercell for 4H-SiC with SF(31) (upper right), and the projected wavefunction along the c-axis, $f(z) = \int\int |\psi(x, y, z)|^2 \, dx \, dy$, for the SF-induced split-off band at the M point (lower right) are shown. Since the supercells are very long along the c-directions, the corresponding first Brillouin zone is almost flat hexagon. In the figure of the localized wavefunction, the normalization integral, $I(z) = \int^z f(z') \, dz'$, is also shown (right-hand scale), together with the corresponding stacking sequence.

respectively, as shown in figure 1. The number of different SFs apparently coincides with the number of different impurity levels associated with substitutional sites in SiC. To the best of our knowledge, the structural differences of these SFs in hexagonal crystals have not been recognized before [3].

We have also investigated multiple SFs in 4H-SiC which can be regarded as CIs [5, 15]. One, two, and three extra SFs are introduced at the neighbouring planes of the already existing SF as shown in figure 1. There also exist different structures in CIs in 4H-SiC. One can start growing CIs both from SF(31) and SF(13) and both in the positive and negative c-directions. This consideration gives a tree diagram for structurally different CIs as shown in figure 1. (The tree diagram for the CIs starting with SF(13) gives almost the same structure.) We have examined the electronic properties and energies of only a subset of all possibilities, namely, the CIs corresponding to one, two, three, and four SFs starting from SF(31) and always in the positive c-directions (i.e., 1SF(31), 2SF(62), 3SF(71), and 4SF(10, 2) in figure 1).

TBs of a type that can be formed without breaking any bonds are also considered here. Apart from the possibility of creating the TBs during crystal growth, it is quite possible to introduce TBs by just pure glide [15]. In terms of the ABC stacking notation, the normal stacking sequence of 3C-SiC is . . . ABCABC . . ., where A, B, and C correspond to Si–C bilayers at A-, B-, and C-sites, respectively, as shown in figure 1. The propagation of a partial dislocation leads to the faulted sequence . . . ABC|BCABCA . . ., where | denotes the slip plane. If still more partial dislocations are introduced immediately above the previous one,

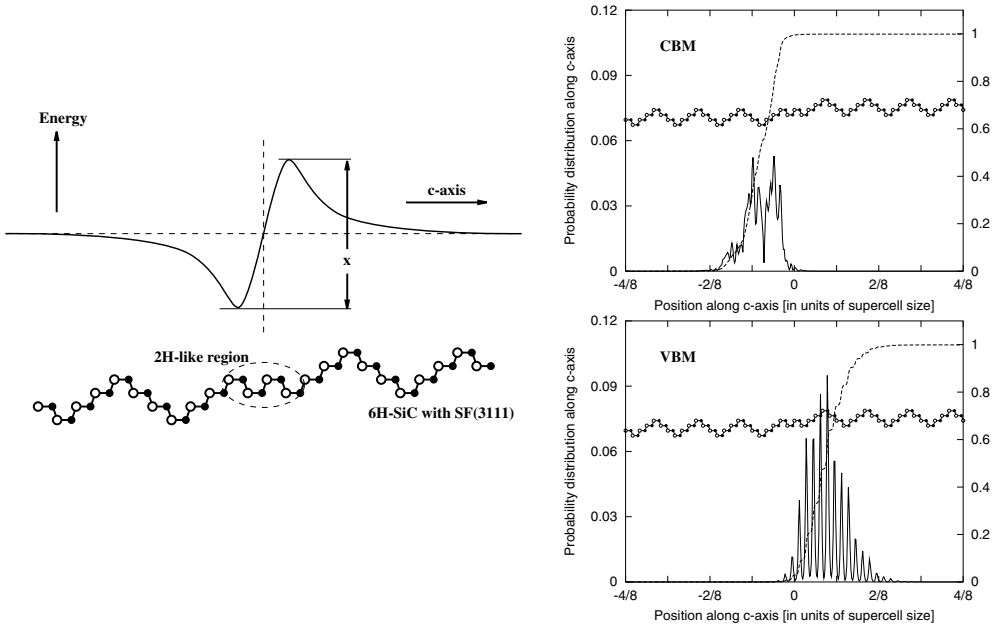

Figure 3. Schematic illustrations of SP features. The SP-induced potential for the SF(3111) in 6H-SiC is drawn schematically (left). The energy height x can be very roughly estimated to be 0.04 eV times the number of hexagonal turns: one for TB in 3C-SiC, two for SF(111) in 3C-SiC, and three for SF(3111) in 6H-SiC and SF(1112) in 15R-SiC. The projected wavefunctions for 6H-SiC with SF(3111) at the bottom of the CB (upper right) and at the top of the VB (lower right) are also shown.

the stacking sequences become . . . ABC|B|ABCAB . . ., . . . ABC|B|A|CABC . . ., and finally . . . ABC|(B|A|C|B|A|C| . . . . . B|A|C)ABC . . .. The stacking sequence in the parentheses is then perfect cubic SiC. Therefore, two TBs are formed in this crystal.

4. Electronic properties and a classification of the planar defects

A striking feature of planar defects in SiC is that cubic-like regions in hexagonal crystals act as QWs for the conduction band (CB) electrons as shown in figure 2. The CBOs between cubic and hexagonal polytypes are very large, e.g., the CBO between 4H (6H) and 3C is about 0.87 (0.64) eV, while the valence band offset (VBO) is around 1/10 of the CBO [13, 16–19]. Therefore, the CB electrons can be confined in the locally lower CB, like for QWs. It has been revealed that SF(31) and SF(13) in 4H-SiC, SF(42) and SF(24) in 6H-SiC, SF(41) and SF(14) in 15R-SiC, and CIs in 4H-SiC give rise to *electrically active* unoccupied states in the fundamental band gap below the CBM, whose wavefunctions are strongly localized perpendicular to the planar defects. These QW-like features can be well confirmed by using a simple rectangular-shape QW model as shown in figure 2 [5, 13]. In contrast to the drastic modification of CBs, VBs are much less sensitive to the occurrence of SFs. The positions of SF-induced split-off bands are listed in table 1. We classify these defects as 'QW class'.

On the other hand, it is found that TBs and SF(111) in 3C-SiC, SF(3111) in 6H-SiC, and SF(1112) in 15R-SiC have very similar features in band structures and wavefunctions, i.e., they give rise to very shallow states in the band gap. The absolute squares of the wavefunctions for the shallow states close to the top of the VB and to the bottom of the CB seem to be localized

Table 1. Positions of the localized band (in eV) below the conduction band minima at the M point in the Brillouin zone. In the case of 3SF(71) and 4SF(10, 2), the second bound states are also seen.

		$n = 1$	$n = 2$
4H-SiC	SF(31)	0.22	—
	SF(13)	0.18	—
6H-SiC	SF(42)	0.19	—
	SF(24)	0.17	—
15R-SiC	SF(41)	0.16	—
	SF(14)	0.11	—
CIs in 4H-SiC	2SF(62)	0.60	—
	3SF(71)	0.71	0.11
	4SF(10, 2)	0.75	0.35

Table 2. Classification of the planar defects. We expect the result for CIs in 4H-SiC to extend to other polytypes.

QW class	SF(31), SF(13), SF(42), SF(24), SF(41), SF(14), CIs
SP class	TBs in 3C-SiC, SF(111), SF(3111), SF(1112)
Inactive class	SF(3322), SF(2233)

almost exclusively on different sides of the planar defects, as exemplified in figure 3. The degree of localization in case of the TBs is the weakest while those in the cases of SF(3111) and SF(1112) are the strongest. We have interpreted this segregation and localization of the wavefunctions close to the band edges as a consequence of the electrostatic field caused by the spontaneous polarization (SP). Qteish *et al* [19] reported that charge transfer takes place between the non-equivalent bonds in the hexagonal SiC polytypes (whereas all four bonds of the tetrahedron in 3C-SiC are equivalent) and results in an electric dipole moment along the negative *c*-direction. Such electric dipole moments are localized around the hexagonal turns. Furthermore, if there is a 2H-like sequence a large electric dipole moment can be created throughout the whole of this 2H-like region with the upper (lower) end negatively (positively) charged. We show schematically in figure 3 the SP-induced potential experienced by an electron around the SF(3111) in 6H-SiC, based on these results. From this figure it is quite understandable that the CB electrons tend to be localized below (to the left of) the 2H-like sequence due to the attractive portion of the potential, and similarly that the electronic state at the top of the valence band is pushed into the band gap by the repulsive part of the potential and gets localized above (to the right of) the 2H-like sequence. We let these four defects belong to the 'SP class'.

Finally, two types of SF in 15R-SiC are left. They do not give rise to localized states in the band gap since neither SF(3322) nor SF(2233) creates 3C- or 2H-like sequences. They are therefore expected to be electrically inactive. We call this group the 'inactive class'.

The classification according to the above-mentioned discussion is summarized in table 2.

5. Stacking fault energies

Stacking fault energies (SFEs) have been calculated using both the supercell method [20] and the ANNNI model (see table 3) [13, 21]. The salient features are:

(1) the SFE in 3C-SiC is negative,

Table 3. SFEs in SiC (in mJ m^{-2}). The values found by the supercell method are calculated without intra-supercell relaxations, i.e., each atomic position is not allowed to displace from its ideal position. We have found that such relaxations have only a small effect (less than around 2 mJ m^{-2}). The geometrical differences were not considered in the experiments.

		Supercell	ANNNI	Experiment [18]	[19]
3C-SiC	SF(111)	−1.71	−6.27		
4H-SiC	SF(31)	17.7	18.2	14.7 ± 2.5	
	SF(13)	18.1	= SF(31)		
6H-SiC	SF(42)	3.10	3.14	2.9 ± 0.6	2.5 ± 0.9
	SF(3111)	40.1	36.6		
	SF(24)	3.35	= SF(42)		
15R-SiC	SF(3322)	0.03	0		
	SF(1112)	38.7	= SF(3111)		
	SF(2233)	0.1	= SF(3322)		
	SF(41)	20.8	21.4		
	SF(14)	20.7	= SF(41)		

(2) in 6H-SiC, the SFE for SF(3111) is considerably larger than those for the other two, and
(3) in 15R-SiC, the SFEs for SF(2233) and SF(3322) are nearly zero while the SFE for SF(1112) is as large as that for SF(3111).

Käckel *et al* [22] also found the SFE in 3C-SiC to be negative. Our calculations are in good agreement with available experimental data [23, 24].

We have also calculated the SFEs for successive SFs for the CIs in 4H-SiC [5]. It is found that the SFE for two SFs in adjacent basal planes is reduced by approximately a factor 4 relative to that for one isolated SF, indicating that double SF structure 2SF(6 2) in 4H-SiC could be quite common. In fact, the rich occurrence of 2SF(6 2) in heavily doped n-type 4H-SiC has been reported by Liu *et al* [12].

Acknowledgments

The authors thank the Swedish Foundation for Strategic Research (SSF) and Ångpanneföreningens Forskningsstiftelse for financial support, as well as the National Supercomputer Centre (NSC), Sweden, for computer time.

References

[1] Lendenmann H, Dahlquist F, Johansson N, Söderholm R, Nilsson P Å, Bergman J P and Skytt P 2000 *Mater. Sci. Forum* **353–356** 727
[2] Bergman J P, Lendenmann H, Nilsson P Å, Lindefelt U and Skytt P 2000 *Mater. Sci. Forum* **353–356** 299
[3] Iwata H, Lindefelt U, Öberg S and Briddon P R 2002 *Mater. Sci. Forum* **389–393** 529
Iwata H, Lindefelt U, Öberg S and Briddon P R 2002 *Phys. Rev.* B **65** 033203
[4] Miao M S, Limpijumnong S and Lambrecht W 2001 *Appl. Phys. Lett.* **79** 4360
[5] Iwata H, Lindefelt U, Öberg S and Briddon P R 2002 *Mater. Sci. Forum* **389–393** 533
Iwata H, Lindefelt U, Öberg S and Briddon P R 2002 *J. Appl. Phys.* at press
[6] Sridhara S G, Carlsson F H C, Bergman J P and Janzén E 2001 *Appl. Phys. Lett.* **79** 3944
[7] Galeckas A, Linnros J, Breitholtz B and Bleichner H 2001 *J. Appl. Phys.* **90** 980
[8] Liu J Q, Skowronski M, Hallin C, Söderholm R and Lendenmann H 2002 *Appl. Phys. Lett.* **80** 749
[9] Bergman J P, Jakobsson H, Storasta L, Carlsson F H C, Magnusson B, Sridhara S, Pozina G, Lendenmann H and Janzén E 2002 *Mater. Sci. Forum* **389–393** 9
[10] Lendenmann H, Dahlquist F, Bergman J P, Bleichner H and Hallin C 2002 *Mater. Sci. Forum* **389–393** 1259
[11] Okojie R S, Xhang M, Pirouz P, Tumakha S, Jessen G and Brillson L J 2002 *Appl. Phys. Lett.* **79** 3056

[12] Liu J Q, Chung H J, Kuhr T, Li Q and Skowronski M 2002 *Appl. Phys. Lett.* **80** 2111
[13] Lindefelt U, Iwata H, Öberg S and Briddon P R 2002 *Phys. Rev.* B submitted
[14] Cheng C, Needs R J and Heine V 1988 *J. Phys. C: Solid State Phys.* **21** 1049
[15] Pirouz P 1997 *Solid State Phenom.* **56** 107
[16] Käckel P, Wenzien B and Bechstedt F 1994 *Phys. Rev.* B **50** 10761
[17] Bechstedt F and Käckel P 1995 *Phys. Rev. Lett.* **75** 2180
[18] Bechstedt F, Käckel P, Zywietz A, Karch K, Adolph B, Tenelsen K and Furthmüller J 1997 *Phys. Status Solidi* b **202** 35
[19] Qteish A, Heine V and Needs R J 1992 *Phys. Rev.* B **45** 6534
Qteish A, Heine V and Needs R J 1992 *Phys. Rev.* B **45** 6376
[20] Chou M Y, Cohen M L and Louie S G 1985 *Phys. Rev.* B **32** 7979
[21] Iwata H, Lindefelt U, Öberg S and Briddon P R 2002 *Mater. Sci. Forum* **389–393** 439
[22] Käckel P, Furthmüller J and Bechstedt F 1998 *Phys. Rev.* B **58** 1326
[23] Hong M H, Samant A V and Pirouz P 2000 *Phil. Mag.* A **80** 919
[24] Maeda K, Suzuki K, Fujita S, Ichihara M and Hyodo S 1988 *Phil. Mag.* A **57** 573